



## Crack growth modes in inhomogeneous materials: analysis of bi- and multi-material interfaces

K. M. Mróz, Z. Mróz

Institute of Fundamental Technological, Polish Academy of Science, Warsaw (Poland)

[kmroz@ippt.gov.pl](mailto:kmroz@ippt.gov.pl) and [zmroz@ippt.gov.pl](mailto:zmroz@ippt.gov.pl)

**ABSTRACT.** Most structural components contain inhomogeneities such as hardened surface layers or coatings, welded or bonded elements, etc. The crack growth mode then depends not only on applied loading and structure geometry but also on material inhomogeneity. In the presentation the analysis of crack growth mode will be discussed for two cases: a bi-material structure with two materials of different thermo-elastic and plastic properties connected along the interface and a structure with introduced interlayer of different material. The simplified approach is presented, namely the *MK*-criterion [1,2] based on the linear elastic fracture mechanics (LEFM). In the criterion it is assumed that crack growth follows the direction of minimum distortion energy density at a distance corresponding to specified value of dilatation energy. For two materials, A and B the crack growth from A to B or along the interface AB may occur depending on relative critical stress and fracture energy values. For a three-phases structure, various modes of crack growth are possible.

**KEYWORDS.** SIF, Strain energy density; LEFM; Fracture; Bi-material; Layers; Fatigue crack growth.

### INTRODUCTION

Recently Mróz et al. [1,2] introduced the new fracture criterion based on the linear elastic fracture mechanics (LEFM) with the energy density divided into two components: distortional energy density  $S_D$  and dilatation energy density  $S_H$ , in a similar way to the familiar *T*-criterion [3]. The components of the strain energy density are expressed, in general, as follows:

$$S = S_D + S_H \quad \text{and} \quad \begin{aligned} S_H &= \frac{(1+\nu^*)^2(1-2\nu)}{6E} (\sigma_{xx} + \sigma_{yy})^2 \\ S_D &= \frac{(1+\nu)}{3E} \left[ (\nu^{*2} - \nu^* + 1)(\sigma_{xx} + \sigma_{yy})^2 - 3(\sigma_{xx}\sigma_{yy} - \sigma_{xy}^2) \right] \end{aligned} \quad (1)$$

where  $\nu^* = 0$  for plane stress,  $\nu^* = \nu$  for plane strain. For the plane strain or stress cases the stress state is expressed in the Cartesian reference system (Fig. 1a) for a homogeneous material as follows:

$$\begin{aligned} \sigma_{yy} &= \frac{K_I}{\sqrt{2\pi r}} A_1 + \frac{K_{II}}{\sqrt{2\pi r}} B_1 & A_1 &= \cos \frac{\theta}{2} (1 + \sin \frac{\theta}{2} \sin \frac{3\theta}{2}), & B_1 &= \sin \frac{\theta}{2} \cos \frac{\theta}{2} \cos \frac{3\theta}{2}, \\ \sigma_{xx} &= \frac{K_I}{\sqrt{2\pi r}} C_1 - \frac{K_{II}}{\sqrt{2\pi r}} D_1 + T_1, & C_1 &= \cos \frac{\theta}{2} (1 - \sin \frac{\theta}{2} \sin \frac{3\theta}{2}), & D_1 &= \sin \frac{\theta}{2} (2 + \cos \frac{\theta}{2} \cos \frac{3\theta}{2}), \\ \sigma_{xy} &= \frac{K_I}{\sqrt{2\pi r}} F_1 + \frac{K_{II}}{\sqrt{2\pi r}} G_1 & F_1 &= \sin \frac{\theta}{2} \cos \frac{\theta}{2} \cos \frac{3\theta}{2}, & G_1 &= \cos \frac{\theta}{2} (1 - \sin \frac{\theta}{2} \sin \frac{3\theta}{2}), \\ & & & & T_1 &= \sigma(1-k) \cos 2\alpha. \end{aligned} \quad (2)$$

The stress field in the crack tip neighbourhood is calculated at a finite distance from the crack tip  $r_c$ . This distance may be considered as a boundary of a region called the core region that contains the severely damaged material undergoing also plastic deformation at the crack tip. Traditionally, the core region can be specified from the critical value of the distortional energy density  $S_D$ , assuming the Huber-Mises yield criterion [3] and then  $r = r_D(\theta)$ .

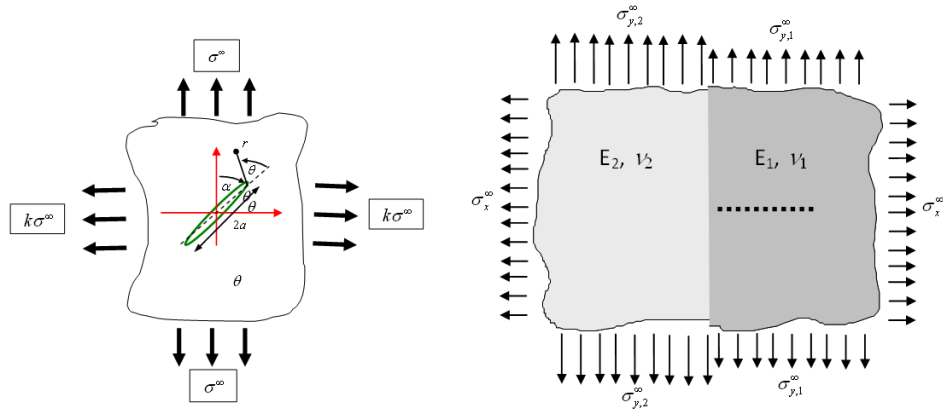


Figure 1: The geometry of the main crack in the homogeneous material and loading of the bimaterial system.

In the neighbourhood of the crack tip also the damage process may occur due to microcracking for the tensile hydrostatic stress. In the case of brittle materials or the high cycle fatigue loading the damage growth is accompanied by a relatively small plastic zone. Assume the size and the shape of the decohesion zone to be related to the hydrostatic stress energy density  $S_H$  of the value specified in terms of the uniaxial ultimate tensile stress  $\sigma_C$  in the following form:

$$S_H = S_H^C = \frac{(1-2\nu)(1+\nu^*)^2}{6E} \sigma_C^2 \quad (3)$$

Basing on this assumption Mróz proposed the MK-fracture criterion postulating that size of damage zone is specified by the condition  $S_H = S_H^C$  and macrocrack propagation follows the direction of smallest plastic dissipation, so it corresponds to a minimum value of the distortional stress energy  $S_D$  specified along the perimeter  $S_H(r, \theta) = S_H^C = \text{const}$ , thus

$$\frac{\partial S_D(r, \theta)}{\partial \theta} = 0 \quad \text{for} \quad S_H(r, \theta) = S_H^C = \text{const} \quad (4)$$

or

$$\left. \frac{S_H}{S_D} \right|_{\max} \rightarrow \theta_{\text{pr}} \quad \text{at} \quad S_H = S_H^C = \text{const.} \rightarrow \left. S_D(r_H(S_H^C, \theta, \alpha)) \right|_{\min} \rightarrow \theta_{\text{pr}} \quad (5)$$

where

$$r_H(S_H^C, \theta, \alpha) = r_H|_{S_H=\text{const}} = \frac{2}{\pi} \left[ \frac{K_I \cos \frac{\theta}{2} - K_{II} \sin \frac{\theta}{2}}{\sqrt{S_H^C \frac{6E}{(1-\nu)(1+\nu^*)^2} - T(\alpha)}} \right]^2 \quad (6)$$

The term under square root can be replaced by the equivalent stress  $\sigma_C$ , so we may write

$$r_H(\sigma_C, \theta, \alpha) = \frac{2}{\pi} \left[ \frac{K_I \cos \frac{\theta}{2} - K_{II} \sin \frac{\theta}{2}}{\sigma_C - T(\alpha)} \right]^2 \quad (7)$$



Consider the particular case of mode I when  $\alpha = \pi/2$  and the crack propagation occurs along the primary crack,  $\theta = 0$ . From (7), it follows that

$$r_H(\sigma_C, 0, \frac{\pi}{2}) = \frac{2}{\pi} \left[ \frac{K_{IC}}{\sigma_C - T(\frac{\pi}{2})} \right]^2 = \frac{2}{\pi} \left[ \frac{K_{IC}}{\sigma_C - \sigma_\infty(1-k)} \right]^2 \quad (8)$$

Assume now, that the critical state is reached on the radius  $r_C = r_{C1} = \text{const}$ . The crack propagation criterion can now be presented as follows

$$K_I \cos \frac{\theta}{2} - K_{II} \sin \frac{\theta}{2} = K_{IC} \frac{\sigma_C - T(\alpha)}{\sigma_C - T(\frac{\pi}{2})} = K_{IC} \frac{\sigma_C - \sigma_\infty(1-k) \cos 2\alpha}{\sigma_C + \sigma_\infty(1-k)} \quad (9)$$

where  $T(\pi/2) = -\sigma_\infty(1-k)$ . This form of the criterion is based on the assumption that mode I is prevailing along the crack path and  $K_{IC}$  is the single crack growth parameter.

## THE INTERFACE PROBLEM

The MK-fracture criterion can be now extended to the crack-interface interaction problem, when the crack propagates in the interface direction and the second material starts to interact with the crack. In this case the extended version of this criterion can be proposed when the effect of second material can be incorporated. The behaviour of propagating cracks in composite materials is, above all affected by the mixed stress field, which results from different boundary conditions and different elastic moduli of composite materials. However, the other important factor is the strength of the materials and interfaces, mainly in the LEFM associated with the critical stress intensity factor ( $K_{IC}$ ).

Let us consider the simple bimaterial case, presented in Fig. 1b. Then the stress component parallel to the interface,  $\sigma_{yy}^\infty$ , for the uniform displacement specified on the sample boundary appears to be discontinuous across the interface line and, based on the condition of strain continuity, the stress  $\sigma_{yy,2}^\infty$  in the material 2 is expressed as follows

$$\sigma_{yy,2}^\infty = \sigma_{yy,1}^\infty \frac{(1-\nu_1^{*2}) E_2}{(1-\nu_2^{*2}) E_1} - \sigma_x^\infty \left( \frac{\nu_1(1+\nu_1^*) E_2}{(1-\nu_2^{*2}) E_1} - \frac{\nu_2}{1-\nu_2^*} \right) \quad (10)$$

Then assuming that the initial crack is located in material 1 (Fig. 1b), in view of Eqs (2) and (10) the component  $\sigma_{yy}$  in material 2 can be expressed as

$$\sigma_{yy,2} = \left( \frac{K_I}{\sqrt{2\pi r}} A_1 + \frac{K_{II}}{\sqrt{2\pi r}} B_1 \right) Y - \left( \frac{K_I}{\sqrt{2\pi r}} C_1 + \frac{K_{II}}{\sqrt{2\pi r}} D_1 + T_1 \right) Z \quad (11)$$

where,  $\sigma_{xx,2} = \sigma_{xx,1}$ ,  $\tau_{xx,2} = \tau_{xx,1}$  on the interface,

$$Y = \frac{(1-\nu_1^{*2}) E_2}{(1-\nu_2^{*2}) E_1},$$

$$Z = \frac{\nu_1(1+\nu_1^*) E_2}{(1-\nu_2^{*2}) E_1} - \frac{\nu_2}{1-\nu_2^*}$$

and  $\nu_1, \nu_2, E_1, E_2$  are the elastic moduli of two materials. Thus we obtained the stress field near the crack tip in both components of bimaterial expressed in terms of the appropriate SIFs. Then, the boundary of the decohesion zone in material 2 can be expressed in the following way:

$$S_{H2} = S_{H2}^C \quad \Rightarrow \quad S_{H2} = \frac{(1 + \nu_2^*)^2 (1 - 2\nu_2)}{6E_2} \sigma_{C2}^2 = W_2 \sigma_{C2}^2 \quad (12)$$

where

$$W_i = \frac{(1 + \nu_i^*)^2 (1 - 2\nu_i)}{6E_i} \quad \text{for } i = 1, 2$$

and

$$\begin{aligned} C_1 + \frac{K_{II}}{\sqrt{2\pi r_{2H}}} D_1 + T_1 + \left( \frac{K_I}{\sqrt{2\pi r_{2H}}} A_1 + \frac{K_{II}}{\sqrt{2\pi r_{2H}}} B_1 \right) Y - \left( \frac{K_I}{\sqrt{2\pi r_{2H}}} C_1 + \frac{K_{II}}{\sqrt{2\pi r_{2H}}} D_1 + T_1 \right) Z = \\ \left( \frac{K_I}{\sqrt{2\pi r_{2H}}} A_1 + \frac{K_{II}}{\sqrt{2\pi r_{2H}}} B_1 \right) Y + \left( \frac{K_I}{\sqrt{2\pi r_{2H}}} C_1 + \frac{K_{II}}{\sqrt{2\pi r_{2H}}} D_1 + T_1 \right) (1 - Z) \end{aligned} \quad (13)$$

Finally, the form of the decohesion zone is expressed as follows

$$\begin{aligned} \frac{1}{\sqrt{2\pi r_{H2}}} = \frac{\sqrt{\frac{S_{HC2}}{W_2}} - T_1(1 - Z)}{K_I(A_1 Y + C_1(1 - Z)) + K_{II}(B_1 Y - D_1(1 - Z))} \Rightarrow \\ r_{2H} = \frac{1}{2\pi} \left( \frac{K_I(A_1 Y + C_1(1 - Z)) + K_{II}(B_1 Y - D_1(1 - Z))}{\sqrt{\frac{S_{HC2}}{W_2}} - T_1(1 - Z)} \right)^2 \Rightarrow \frac{1}{2\pi} \left( \frac{K_I(A_1 Y + C_1(1 - Z)) + K_{II}(B_1 Y - D_1(1 - Z))}{\sigma_2^C - T_1(1 - Z)} \right)^2 \end{aligned} \quad (14)$$

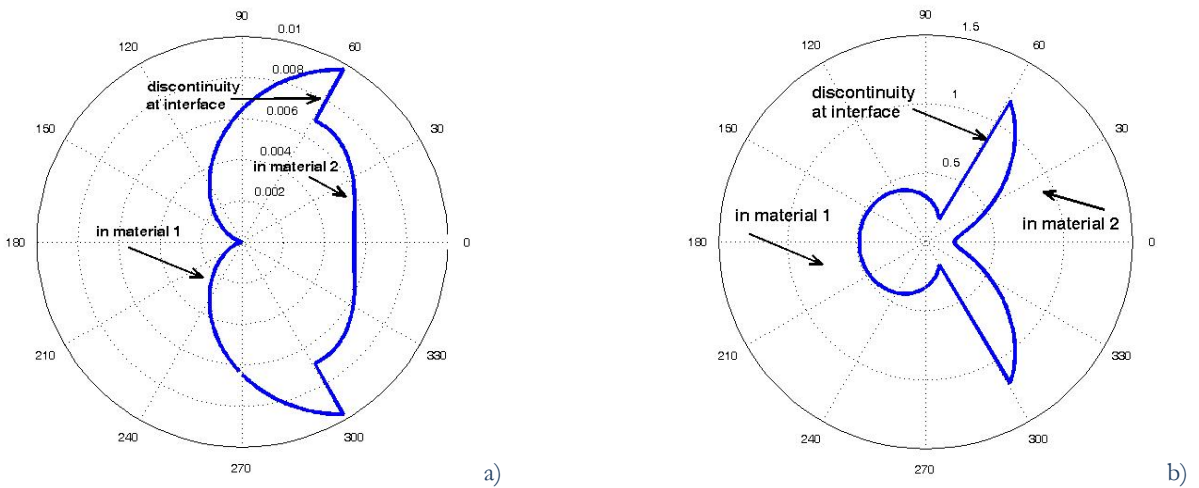


Figure 3: The contours of  $S_D(r_{Hl})$  and  $S_H = \text{const.}$  for  $E_2 = 128 \text{ GPa}$ ,  $E_1 = 64 \text{ GPa}$ ,  $\sigma_{C1} = 300 \text{ MPa}$ ,  $\nu_{1,2} = 0.33$ ,  $\sigma_{C2} = 500 \text{ MPa}$ ,  $\sigma_{APL} = 100 \text{ MPa}$ ,  $\alpha = 0$ ,  $2a = 0.2$ ,  $d = 0.005$ . (a) the decohesion zone,  $r_{Hl}(\theta, S_{HC})$ , (b) the contour of distortional energy density,  $S_D(r_{Hl})$  in two materials. The global minimum of the distortional part is located at  $\theta = \pm 59.5^\circ$ .



The MK-criterion in form (5) is valid for the crack near the bimaterial interface, if the whole and appropriate decohesion zone is considered (Fig. 2). So, there is

$$S_{Di}(r_{Hi}(S_{Hi}^C, \theta)) \Big|_{\min} \rightarrow \theta_{pr}, \quad \text{for } i=1,2 \quad i=(1,2) \quad (15)$$

with the additional condition:

$$\theta_{PR} \leftarrow \max \left( \frac{r_V^A(\theta_A)}{r_{VCr}^A}, \frac{r_V^B(\theta_B)}{r_{VCr}^B} \right) \quad (16)$$

Figs. 2a and 3a present the decohesion zone in the bimaterial for crack ( $a=0.2$ ) located in material 1 perpendicularly to the interface with its left tip at distance  $d_0=0.005$  to the interface. The crack is loaded perpendicularly to the surface. Comparing Tables 1 and 2, it can be seen that more important effect on the crack growth angle is exhibited by the distance of crack tip to the interface than by the difference of Young moduli.

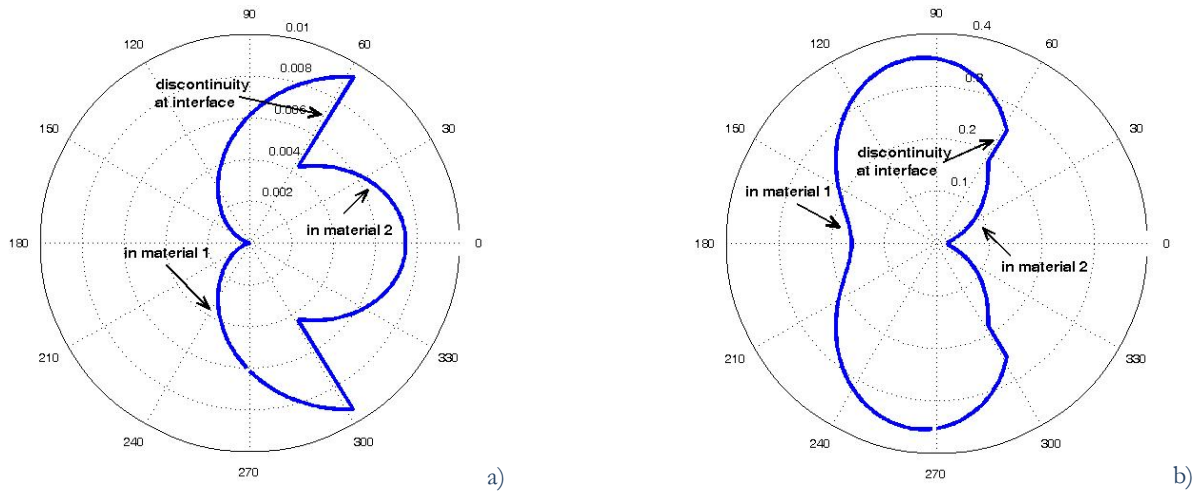


Figure 3: The contours of  $S_D(r_H)$  and  $S_H = \text{const.}$  for  $E_1 = 192 \text{ GPa}$ ,  $E_2 = 128 \text{ GPa}$ ,  $\nu_{1,2} = 0.33$ ,  $\sigma_{C1} = 200 \text{ MPa}$ ,  $\sigma_{C2} = 500 \text{ MPa}$ ,  $\alpha = 0$ ,  $2a = 0.2$ ,  $d = 0.005$ . (a) the decohesion zone,  $r_{Hi}(\theta, S_{Hi})$ , (b) the contour of distortional energy density,  $S_D(r_{Hi})$  in two materials. The global minimum of the distortional part is located at  $\theta_{pr} = 0^\circ$ .

$E_1/E_2$	2	1.5	1	0.8	0.6	0.5	0.4	0.3	0.2	0.1	0.05
$\pm\theta_{pr} [^\circ]$	0	0	0	0	0	59.5	59.6	60	60.5	61.5	61.55

Table 1: The predicted crack growth angles for different ratios of  $E_1/E_2$ . The material and geometrical parameters are the same as in Fig.2.

$d_0$	0.015	0.0012	0.0010	0.0008	0.0005
$\pm\theta_{pr} [^\circ]$	0	0	28.5	42	59.5

Table 2: The predicted angles of crack propagation for different distances of left crack tip to the interface for  $E_1/E_2 = 0.5$ .

## CRACK INTERACTION WITH THE MATERIAL INTERLAYER

Recently, the effect of plastic mismatch on crack propagation in bonded materials with a finite thickness interlayer (Fig. 4) or bimaterial, was analyzed in several papers [4 - 7]. It is assumed that elastic moduli of materials are the same but yield and ultimate stresses are different (plastic mismatch). In Fig. 4, the specific case is considered,

when the crack propagates perpendicularly to the interlayer of small thickness  $t$  in the matrix material. The elastic and thermal expansion properties of the interlayer are nearly identical and only plastic properties and ultimate stresses are different. The experimental studies exhibited the effect of plastic mismatch on crack penetration near the interface [4,8,9,10] and we refer to the analysis of Pippan et al. [10] who studied the growth of fatigue crack approaching the interface in a bimaterial and in a material with interlayer. The weaker ARMCO-iron ( $\sigma_{YS}^A = 140[\text{MPa}]$ ,  $\sigma_{UTS}^A = 228[\text{MPa}]$ ) and the plastically stronger SAE 4340 steel ( $\sigma_{YS}^S = 530[\text{MPa}]$ ,  $\sigma_{UTS}^S = 672[\text{MPa}]$ ) were used as model components. The classical criteria of fracture mechanics cannot be applied to the case when two materials have the same elastic moduli but different yield stresses. Two types of interlayers are considered, namely a weak interlayer in a strong material and a plastically strong interlayer in a weak matrix. For both types of specimens with interlayers, the interlayer thicknesses are different, namely  $t = 100 - 150[\mu\text{m}]$  in the first case and  $t = 250 - 350[\mu\text{m}]$  in other case. All fatigue tests were performed at constant far field  $\Delta K$ . To keep  $\Delta K$  constant, the load amplitude and the mean load were adjusted in steps after each crack extension of about 0.3 mm. The three values  $\Delta K$  were applied, namely  $\Delta K = 10, 18$  and  $20 [\text{MPa}\sqrt{\text{m}}]$  as they satisfy the threshold conditions of the stress intensity range.

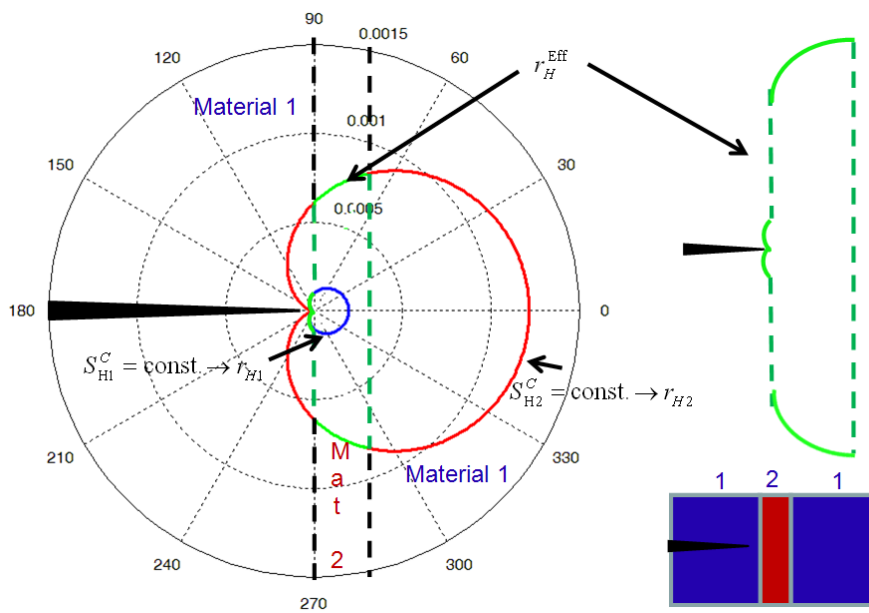


Figure 4: The sketch of the damage areas, according to decohesion criterion for SM-WI boundary specimen.

The present model can be thus applied to the four scenarios of the crack propagating from:

- the plastically weaker material (WM) to the plastically stronger material (SM), WM-SM,
- the plastically weaker material (WM) to the plastically stronger interlayer (SI), WM-SI,
- the plastically stronger material (SM) to the plastically weaker material (WM), SM-WM,
- the plastically stronger material (SM) to plastically weaker interlayer (WI), SM-WI.

The most interesting cases are related to the crack-interlayer interaction when three portions of materials are bonded together. Fig. 4 presents the forms of damage contours predicted by Eqs (7) and (14) for the case of SM-WI specimen. The effective contour  $r_H^{\text{Eff}}$  is composed of two portions with discontinuity variation at the interface. The damage contour  $r_{H1}$  corresponding to  $S_{H1}^C = \text{const.}$  starts in the material 1 and ends at the left interface. The damage contour of interlayer  $r_{H2}$  starts at the left interface and corresponds to much higher values of  $r_{H2}$ . The minimum of  $S_D(r)$  specified on the  $r_H^{\text{Eff}}$  composed of two portions provides the crack growth orientation angle. Referring to Pippan et al. [10] it was observed that for crack penetration from stronger to weaker material, the fatigue crack bifurcates near the right interface within the interlayer at smaller stresses amplitude and near the left interface at larger stress amplitude. This effect can be interpreted by the present model. Fig. 5 presents the case of SM-WI and illustrates the crack path bifurcation for two different stress amplitudes,  $\Delta K = 10$  and  $20 \text{ MPa}\sqrt{\text{m}}$ . Fig. 6 presents the opposite case of weak material-strong interlayer (WM-SI). In this case the decohesion contour of weak material controls the crack growth orientation, namely along the



left interface. Depending on the distance of crack tip the the left interface, and on the interlayer thickness  $t$ , the curvilinear path is generated, tending to the parallel orientation to the interface. This effect is supported by experimental observation of Ref. [10], cf. Fig. 6. Let us note that the damage contour of weak material  $r_{H1}$  on the right side of the interlayer does not affect the crack orientation growth. However, the damage zone effects of both materials should be accounted for in the crack growth conditions due to energy dissipation in this zone.

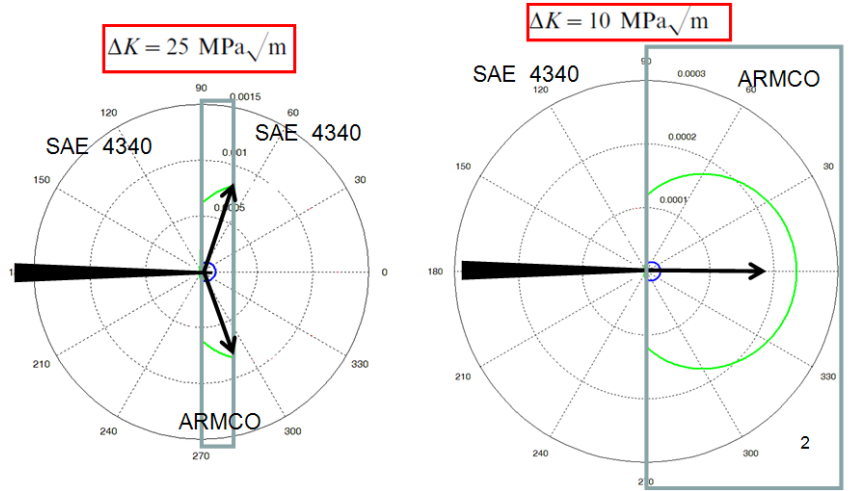


Figure 5: The sketch of the damage areas, according to decohesion criterion for SM-WI boundary specimen. The crack growth orientation for (a) 25 [MPa√m], (b) 10 [MPa√m].

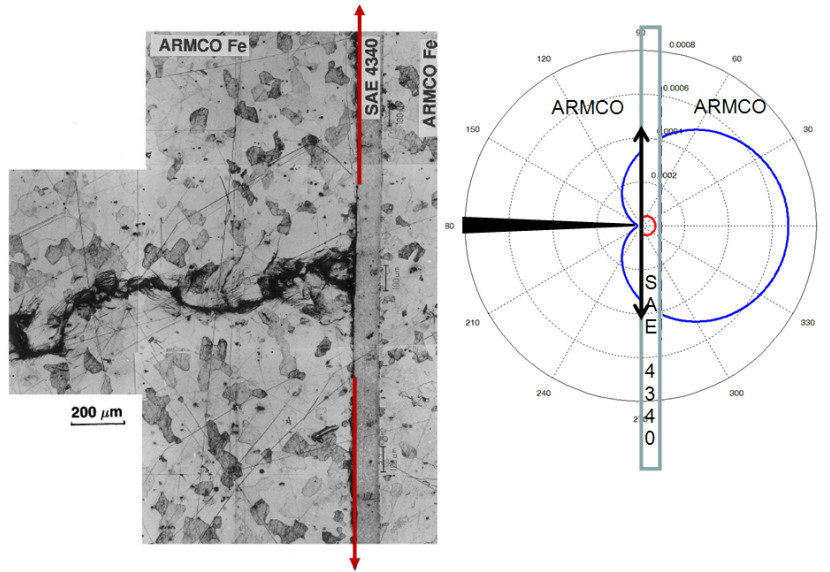


Figure 6: Optical macrograph and sketch of bifurcation of the crack, based on Ref. [10] for  $\Delta K = 18$  [MPa√m]. The arrows indicated the crack growth directions.

Classically, the crack growth conditions for through-thickness central crack of length  $2a$  is associated with Griffith's theory in simple formula based on the total elastic energy of a cracked plate:

$$U_t = \int_A \frac{\sigma^2}{2E} dA \pm \frac{\pi\sigma^2 a^2}{E} + \int_{\delta} F dy + 4a\gamma_e \quad (17)$$

where  $F$  is the applied force per unit thickness,  $\delta$  is the total relative displacement of loaded boundaries,  $\gamma_e$  is the surface energy of the material per unit thickness and physically is equivalent to energy required to break two atomic bonds ahead



of the crack tip. The second part of Eq. (17) is associated with the elastic energy released by the introduction of crack of length  $2a$ . However, Irwin [11,12] and Orowan[13] postulated extended form of Griffith theory to account for the plastic dissipation ahead of the crack tip. In present analysis the damage dissipation is approximated by the hydrostatic part of the strain energy density in the whole damage zone specified by  $r_{Hi}$  ( $i=1,2,3$ ). For the Mode I and for  $T=0$  the dissipated decohesion energy for homogeneous materials is given by

$$G_H^D = 2 \int_{-\pi}^{\pi} \int_0^{r_i} \frac{(1-2\nu)(1+f)^2}{6E} \left( \frac{2K_I}{\sqrt{2\pi r}} \cos \frac{\theta}{2} \right)^2 r dr d\theta = \frac{(1-2\nu)(1+\nu^*)^2}{E\pi} \frac{K_I^4}{\sigma_C^2} \quad (18)$$

then

$$U_t = \int_A \frac{\sigma^2}{2E} dA \pm \frac{K_I^2 a}{E} - \frac{(1-2\nu)(1+\nu^*)^2}{E\pi} \frac{K_I^4}{\sigma_C^2} + \int_s F dy + 4a\gamma_e \quad (19)$$

Under the fixed grip conditions there is

$$\frac{\partial U_t}{\partial a} = \frac{\partial}{\partial a} \left( - \left( \frac{K_I^2 a}{E} - \frac{(1-2\nu)(1+\nu^*)^2}{E\pi} \frac{K_I^4}{\sigma_C^2} \right) + 4a\gamma_e \right) = 0 \quad (20)$$

and then

$$K_I \sqrt{1 - \frac{(1-2\nu)(1+\nu^*)^2}{a} \frac{K_I^2}{\sigma_C^2}} = \sqrt{2\gamma_e E} \quad (21)$$

For the bimaterial the crack growth condition is stated as follows

$$K_I \sqrt{1 - f(S_1) \frac{(1-2\nu)(1+\nu^*)^2}{a} \frac{K_I^2}{\sigma_{C1}^2} - g(S_2) \frac{(1-2\nu)(1+\nu^*)^2}{a} \frac{K_I^2}{\sigma_{C2}^2}} = \sqrt{2\gamma_e E}$$

where  $f(S_1)$  and  $g(S_2)$  depend on the damaged areas, respectively for material 1 and 2.

## CONCLUSION

The presented analysis is aimed at application of the energy MK-criterion to predict crack growth orientations and critical load condition in inhomogeneous materials. The model application was illustrated by application to crack growth in a bi-material system and material-layer system. In both cases the crack growth orientations confirm qualitatively the model predictions.

## REFERENCES

- [1] K.P. Mróz, Z. Mróz, Engineering Fracture Mechanics, 77 (2010) 1781.
- [2] K.P. Mróz, K. Doliński, Z. Angew. Math. Mech, 90 (2010) 721.
- [3] P. S. Theocaris and N. P. Andrianopoulos, Eng. Fract. Mech. , 16 (1982) 425.
- [4] Y. Sugimura, P.G. Lim, C.F. Shih, S. Suresh, Acta metal. Mater., 43(3) (1995) 1157.
- [5] T. Siegmund, N.A. Fleck, A. Needleman, International Journal of Fracture, 85 (1997) 381.
- [6] R. Pippa, F.O. Riemelmoser, Computational Materials Science, 13 (1998) 108.
- [7] A. S. Kim, S. Suresh, Int. J. Solids Structures, 34 (1997) 3415.
- [8] S. Suresh, Y. Sugimura, E. K. Tschegg, Scripta Metallica Materiala, 27 (1992) 1189.





- [9] S. Suresh, Y. Sugimura, T. Ogawa, *Scripta Metallica Materiala*, 29 (1993) 237.
- [10] R. Pippan, K. Flechsig, F. O. Riemelmoser, *Materials Science and Engineering*, A283 (2000) 225.
- [11] G.R. Irwin, *Fracturing of Metals*, ASM, (1955) 147.
- [12] G. R. Irwin, J. Kies, *Welding J. Res. Suppl.*, (1952)
- [13] E. Orowan, *Welding J.*, 34 (1955) 1575.